

## COMMISSIONING AND PERFORMANCE OF LCLS CAVITY BPMS \*

Stephen Smith, Sonya Hoobler, Ronald G. Johnson, Till Straumann, Andrew Young, SLAC National Accelerator Laboratory, Menlo Park, CA 94025, U.S.A.

Robert M.Lill, Leonard H. Morrison, Eric Norum, Nicholas Sereno, Geoff J. Waldschmidt, Dean Walters, Argonne National Laboratory, Argonne, IL 60439, U.S.A.

### Abstract

The Linac Coherent Light Source (LCLS) is a free-electron laser (FEL) at SLAC producing coherent 1.5 Angstrom x-rays. This requires precise, stable alignment of the electron and photon beams in the undulator. We describe here the beam position monitor (BPM) system which allows the required alignment to be established and maintained. The X-band cavity BPM employs a  $TM_{010}$  monopole reference cavity and a  $TM_{110}$  dipole cavity designed to operate at a center frequency of 11.384 GHz. Processing electronics feature low-noise single-stage three-channel heterodyne receivers with selectable gain and phase-locked local oscillator. System requirements include sub-micron position resolution for a single-bunch beam charge of 200 pC. We discuss the specifications, commissioning and performance of 36 installed BPMS. Single shot resolutions have been measured to be approximately 200 nm rms at a beam charge of 200 pC.

### REQUIREMENTS

To reach laser saturation in the LCLS FEL, the electron and photon beams must be collinear in the 131 meter-long undulator to about 10% of the  $\sim 37 \mu\text{m}$  rms transverse beam spot size on scales of the FEL amplitude gain length ( $\sim 4\text{m}$ ) [1,2]. BPM system design requirements include centering accuracy, reproducibility, small physical size radiation hardness, and submicron resolution at 200 pC.

### SYSTEM DESIGN

The major subsystems for the LCLS undulator BPM system are the cavity BPM, receiver, and data acquisition components. The cavity BPM and downconverter reside in the tunnel and the analog-to-digital converters (ADC) are located in surface buildings.

Thirty-four BPMS are installed on undulator girders while two are placed in the linac-to-undulator (LTU) transport line[3]. The BPMS provide stable and repeatable beam position data for both planes on a pulse-to-pulse basis for up to a 120-Hz repetition rate.

#### X-Band Cavity Design

The two-cavity BPM design shown in Figure 1 illustrates the electric field vectors simulated when the beam is offset[4]. The beam passes through the monopole reference cavity, shown on the right, exciting the  $TM_{010}$  monopole mode signal resonant at 11.384 GHz. The monopole mode signal is proportional to the beam charge. The dipole cavity is located 36 mm downstream through

the 10-mm-diameter beam pipe. Isolation between the monopole cavity and the dipole cavity is 130 dB, governed by the decay of the fields due to the below-cutoff beampipe, copper losses, and poor coupling of the TM beampipe mode to the cavity dipole mode.

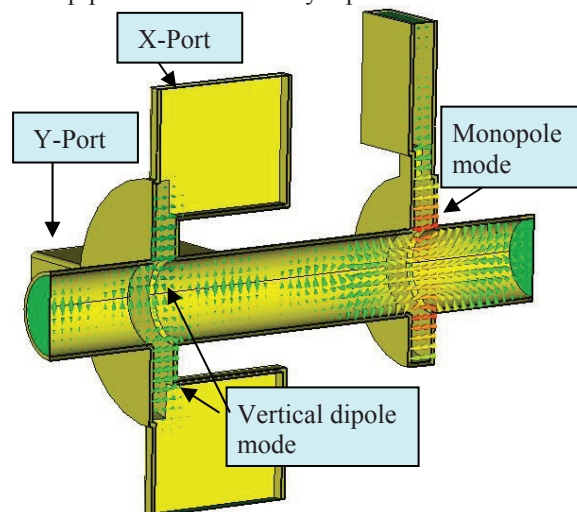


Figure 1: BPM Cavity schematic with electric fields of position (dipole) and reference (monopole) cavities.

The downstream (position) cavity has its  $TM_{110}$  dipole mode resonant at 11.384 GHz. Its output is proportional to the product of beam position times bunch charge. The X and Y position modes are nominally degenerate in frequency, with the appropriate component chosen by the geometry of the couplers. The dipole coupler geometry is chosen to reject (larger) monopole modes[5-7].

The iris couplers are precisely electrical discharge machined (EDM) into a solid copper block to ensure repeatable and accurate coupling. This technique ensures that the waveguide braze has little or no effect on the cavity performance from the migration of braze material. The dipole cavity was designed as a 4-port device, two opposing X couplers orthogonal to two opposing Y couplers. This is useful for cold testing and preserves symmetry. The unused ports are terminated with the potential for using them for future diagnostics.

Forty BPMS were built to a tolerance of  $\pm 10$  MHz of design frequency. To accomplish this without demanding unrealistic machining tolerances a tuning process was developed. The first tuning step is executed after the parts are inspected and cleaned. End caps are fitted into the body and clamped to a test fixture. The center frequency and bandwidths are measured, then micro-machining is performed on the end cap beam pipe inner diameters. The end caps are reassembled and tested again to ensure the

\* Work supported by U.S. Department of Energy under Contract Numbers DE-AC02-06CH11357 and DE-AC02-76SF00515.

cavities are within the tolerance of +0, -10 MHz to compensate for frequency shift in the brazing process. The end cap brazing was strictly controlled and a 10 MHz frequency shift was typically measured after the braze.

The dipole cavity final tuning was accomplished using a sliding hammer in up to eight boss locations in the endcap to dimple the wall of the cavity. Four tuners in-line with the iris couplers are used for frequency

adjustment. These tuners reduce the resonant frequency when inserted. Four cross-talk tuners on the dipole cavity end cap are located at 45 degrees to the iris couplers. They reorient the dipole mode such that the modes are symmetric about the vertical and horizontal planes. These tuners are used to set the symmetry of the modes and optimize the isolation between planes.

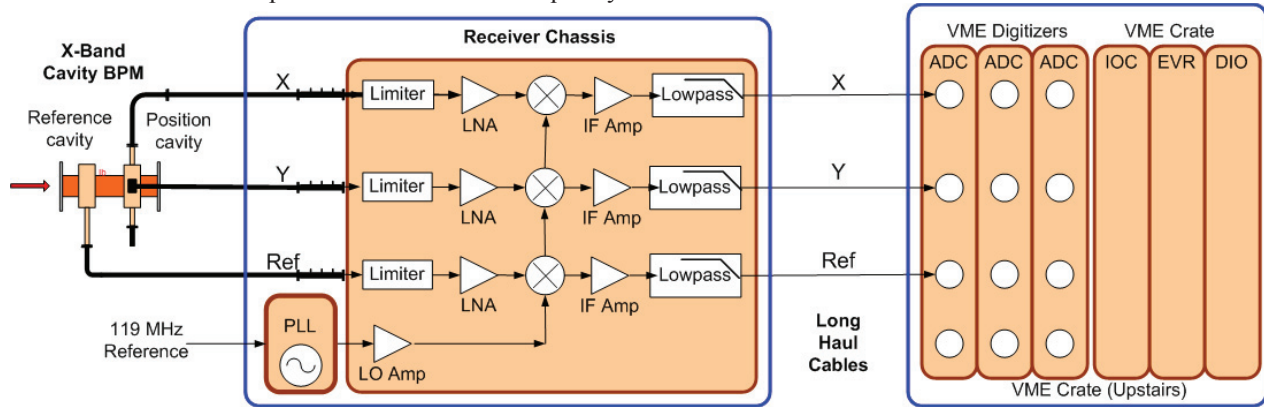


Figure 2: System block diagram. The receiver is mounted on the undulator stand while the digitizers are upstairs.

### Receiver

An in-tunnel, three-channel, single-stage heterodyne receiver (Figure 2) downconverts incoming X-band signals to an intermediate (IF) frequency in the range 25-50 MHz. Each of the receiver inputs is limited to a 3 dB bandwidth of 35 MHz around 11.384 GHz. The filters also provide a broadband -10 dB return loss match to the cavities. Out-of-band filtering of -60 dB prevents higher modes from saturating the receiver input. The signals are first amplified in a low noise amplification (LNA) stage, then translated to a lower IF by mixing with a local oscillator (LO). The LNA is protected against high-power surges by a limiter that is rated at 50 W peak. The dynamic range of the electronics is extended by switching the gain of the receiver. The overall conversion gain/loss is +10 dB in the high gain mode and -15 dB in low gain mode. The LO is a low noise phase-locked dielectric resonant oscillator (PDRO). The LO is locked to the 119-MHz timing reference [8].

### Digitizer

The X, Y, and Reference signals are digitized to 16 bits at 119 MHz sampling rate in 4-channel VME digitizers designed and built at SLAC. Waveforms are transmitted over the VME backplane to a VME processor which reduces waveforms to beam position and charge.

## ALGORITHM

Beam charge at each BPM is estimated by scaling the amplitude of the reference cavity. Each position waveform is reduced to amplitude and phase in an appropriate bandwidth around the cavity frequency. Normalized amplitudes are formed by dividing by the amplitude of the reference cavity and rotating by its phase. Position is estimated by rotating this complex

normalized amplitude by a phase established with beam calibration, projecting out the position component, and scaling to microns. Finally a linear transformation accounts for potential physical rotations of the BPM, non-orthogonality of the X and Y ports, and coupling between the ports.

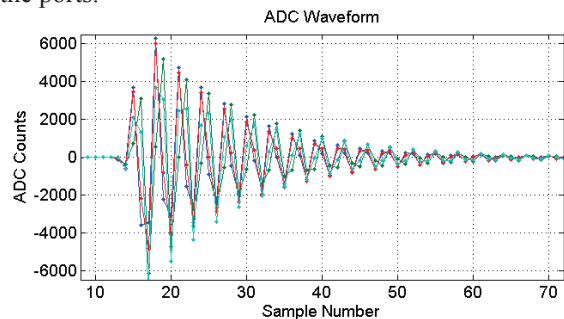


Figure 3: BPM raw waveforms sampled at 119 MHz.

## CALIBRATION

Recovering beam position and charge from the digitized cavity waveforms requires knowledge of cavity phases and scales. Undulator BPMs are calibrated for position response by mechanically moving the girder on which the BPM is fixed, fitting the phase and amplitude of the position cavity signals normalized in phase and amplitude to the reference cavity. Presently the production BPM code calibrates by moving BPMs in 100 micron steps, much larger than typical 10 to 20 micron beam jitter. In principle we can use uncalibrated measurements from nearby BPMs to remove beam jitter during calibration, and therefore calibrate with motion below alignment tolerances. The results of such a small-move calibration are shown in Figure 4. Transfer line BPMs, which are not mounted on movers, are calibrated

### Instrumentation

by moving the beam with respect to the BPM using an upstream corrector.

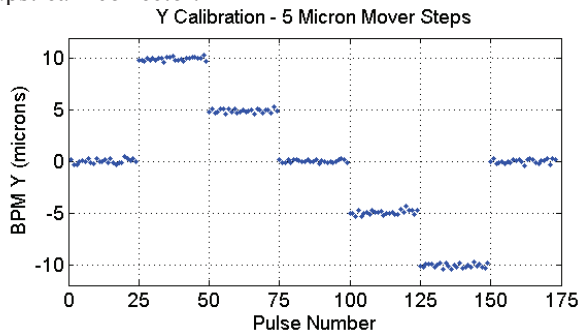


Figure 4: Calibration moving BPM in 5 micron steps.

## PERFORMANCE

### Resolution

We evaluate sub-micron BPM resolution in the presence of >10 micron beam jitter by acquiring beam position synchronously over many beam pulses from many BPMs. A least-squares fit predicts position in each BPM as a linear combination of position measured in neighboring BPMs. Figure 4 shows this procedure applied to the 26th cavity BPM. It shows Y measured 120 times in 3 adjacent BPMs, measured Y versus that predicted from four closest neighbors, and the fit residual, or difference between measurement and prediction. The scatter of fit residual is taken as an estimate of BPM resolution. Also plotted is the histogram of Y resolutions measured this way for 33 BPMs.

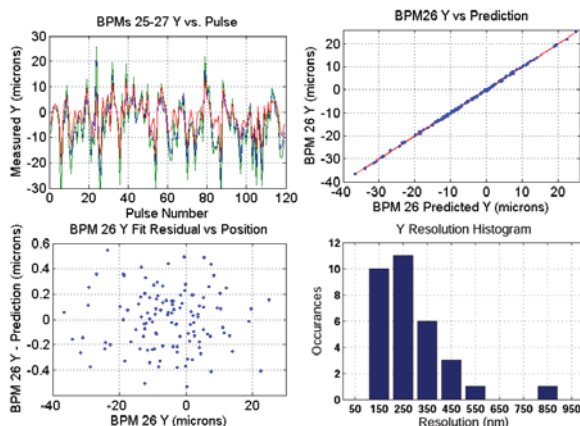


Figure 5: Upper-left: Y position measured at adjacent BPMs for 120 pulses. Upper right: Y at BPM26 vs. best fit prediction from its neighbors. Lower left: Fit residual, Lower right: Histogram of measured BPM resolutions.

### Stability

We evaluate two aspects of BPM stability. Calibration stability is evaluated by repeated calibrations, taken about once per shift (8 hours) over three days. We find the scale drifting by less than 0.5% per 24 hours and the phase stable to 0.1 degree.

Secondly we record groups of about 100 beam pulses every 20 minutes over a 3.5 day period using a single calibration. Using adjacent BPMs to remove beam jitter, we plot measured beam position at each BPM. Typical stability is better than 1 micron drift over 24 hours. Figure 6 show drift in a typical BPM.

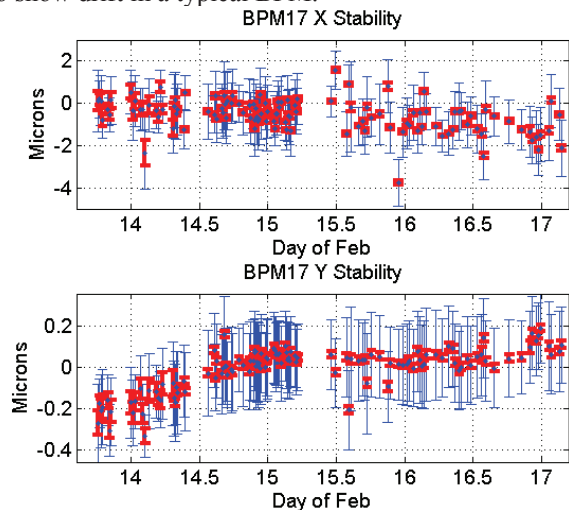


Figure 6: Position stability for a BPM over days. Each dot is the mean measured position for ~100 pulses after beam jitter removal. Blue error bars represent the rms spread of position, red bars are the expected error of the mean.

## REFERENCES

- [1] R. Hettel, R. Carr, C. Field, and D. Martin, "Investigation of Beam Alignment Monitor Technologies for the LCLS FEL Undulator," BIW98, Stanford CA, May 1998, p. 413.
- [2] P. Emma, J. Wu, "Trajectory Stability Modeling and Tolerances in the LCLS," EPAC06, Edinburgh, Scotland, June 2006, p. 151.
- [3] R. Lill, G. Waldschmidt, D. Walters, L. Morrison, S. Smith, "Linac Coherent Light Source Undulator RF BPM System," FEL06, Berlin, Germany, July 2006, p. 706.
- [4] G. Waldschmidt, R. Lill, L. Morrison, "Electromagnetic Design of the RF Cavity Beam Position Monitor for the LCLS", PAC 07, Albuquerque NM, May 2007, p. 1153.
- [5] V. Balakin, "Experimental Results From a Microwave Cavity Beam Position Monitor", PAC99, New York, May 1999, p. 461.
- [6] Z. Li, et al "Cavity BPM with Dipole-Mode-Selective Coupler", PAC03, Portland OR, May 2003, [http://accelconf.web.cern.ch/AccelConf/p03/PAPER\\_S/ROAB004.PDF](http://accelconf.web.cern.ch/AccelConf/p03/PAPER_S/ROAB004.PDF).
- [7] S. Walston, et al, "Performance of a High Resolution Cavity Beam Position Monitor System." NIM A578, 2007.
- [8] R. Lill, G. Waldschmidt, D. Walters, L. Morrison, S. Smith, "Design and Performance of the LCLS Cavity BPM System", PAC07, Albuquerque NM, p. 1153.